Human cortical areas are sparsely connected: Combining histology with diffusion MRI to estimate the absolute number of axons

Burke Q. Rosen[a,1] Eric Halgren[a,b]

[a]Neurosciences Graduate Program, University of California, San Diego, La Jolla CA 92093
[b]Depts. of Neurosciences & Radiology, University of California, San Diego, La Jolla CA 92093
[1]bqrosen@health.ucsd.edu
3510 Dunhill St.
San Diego, CA 92101
858-405-9660

The tracts between cortical areas are conceived as playing a central role in cortical information processing, but their actual numbers have never been determined. Here we estimate the absolute number of axons linking cortical areas from a whole-cortex diffusion-MRI (dMRI) connectome, calibrated using the histologically-measured callosal fiber density. Median connectivity is estimated as ~2,700 axons between cortical areas within-hemisphere and ~540 axons interhemispherically, with axons connecting functionally-related areas surprisingly sparse. These results challenge models that require direct transmission of detailed information between cortical areas, rather suggesting that cortical integration mainly relies on the extremely dense local connections.

The major tracts connecting cortical areas have long been central to models of information-processing in the human brain (1). Such models have been refined and applied to development and disease with the advent of diffusion-MRI (dMRI) (2). However, dMRI only provides *relative* connectivity, not the absolute number of axons. Relative connectivity is very useful in many circumstances but more constraints would be possible if the absolute number of axons connecting different cortical areas could be estimated. We find that routinely observed widespread functional synchronization belies a surprising small absolute number of long range axons connecting functionally-related areas.

The basic principle of our method is very simple. Given a dMRI-based measure of total interhemispheric connectivity in arbitrary units and the physical number of axons traversing the corpus callosum, the conversion factor between the two can be obtained by dividing the first by the second. Specifically, we started with the total interhemispheric tractography strength reported in our dMRI connectome of the Human Connectome Project (HCP) cohort (3). For each individual, the cross-sectional area of the corpus callosum was obtained using the standard FreeSurfer structural MRI pipeline (4). Multiplying this number by a histologically ascertained callosal fiber density (5) yields an estimate of the number of axons traversing an individual's corpus callosum. Dividing this count by individuals' interhemispheric dMRI streamline value yields the conversion ratio from the arbitrarily-scaled dMRI metric to the absolute number of axons. Note that this procedure does not at all depend on the scale of the dMRI metric, requiring only that it be proportional to absolute number of fibers. Therefore, while the ratio itself is study-specific, the procedure can be applied to any dMRI tractography method or parameter set. It only requires that the dMRI method return a continuous distribution of connectivity values and have reasonably similar sensitivity to colossal and ipsilateral fiber tracts.

Our previous dMRI study (3) includes estimated tractography streamlines among all 360 parcels of the HCP-MMP1.0 atlas (6) for each of the 1,065 individuals in the HCP dMRI cohort. The sum connectivity between the 180 left hemisphere cortical parcels and the 180 right (180^2 parcel pairs) constitutes the total callosal connectivity, on average 1.25×10^8

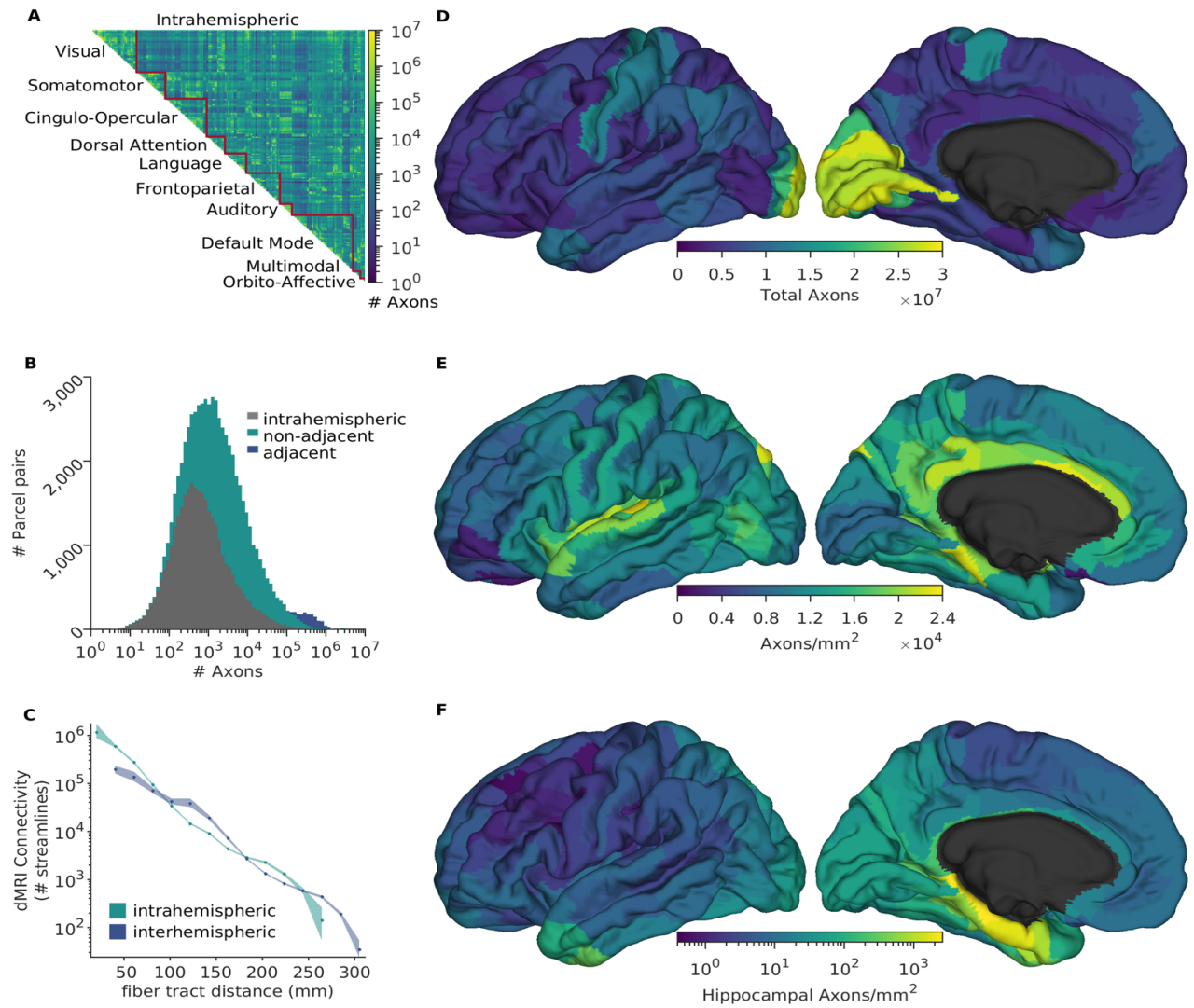

Fig. 1. The number of axons connecting interconnecting the 360 cortical parcels of the HCP-MMP1.0 atlas. (A) Connectivity matrix of intrahemispheric axon counts, averaged across the two hemispheres. Parcels are ordered into 10 functional networks. (B) Stacked histogram showing the distribution of inter- and intrahemispheric pairwise axon counts, with the contributions of physically adjacent parcel pairs indicated. Median connectivity is ~2,700 axons between cortical areas in the same hemisphere, and 540 interhemispherically. (C) dMRI connectivity as a function fiber tract distance. Pairwise values averaged within 15 fiber-length bins. Shading shows bootstrapped 95% confidence intervals. (D-F) axons counts and densities averaged across the two hemispheres and visualized on the left fsaverage template cortex. (D) total axons connecting each parcel to all others. (E) axons connecting each parcel to all others, normalized by the reference parcel's area. (F) axons connecting the hippocampus to the rest of the cortex, normalized by the area of the cortical parcel, shown in log scale.

streamlines. Based on our assumed fiber density ($1.6x10^5$ axons/mm^2) (5) and measured callosal cross-sectional area (mean = 689.45mm^2), we estimate this cohort to have an average of $1.1x10^8$ callosal fibers. The mean quotient between these two quantities is 0.87 axons-per-streamline, a ratio specific to the dMRI methodology and parameters used.

Applying the conversion factor to the inter-parcel connectivity from our prior study yields an estimate of the absolute number of axons connecting different cortical areas (Fig. 1*A*), $1.05x10^9$ axons in total. Axons are approximately log-normally distributed among non-adjacent parcel pairs, with adjacent pairs having disproportionally high axon counts (Fig. 1*B*). The total count of a parcel's axons to or from all other areas is much less variable when normalized by the parcel's area (Fig. 1 *D* and *E*). Multiplying the total number of fibers by the effective fiber cross-sectional area (the inverse callosal packing density, $6.2x10^{-6}$ mm^2/axon) yields $6.6x10^3$ mm^2 of cortex or 3.7% of the total white-gray interface. Note that the effective axonal area includes myelin, supporting cells and intercellular space in addition to the axon proper. The percent of fiber-allocated cortical area is quite similar to the ~4% of total cortical fibers Shülz and Braitenburg estimated (7) are contained in the corpus callosum and long fascicles. The remaining ~95% of cortical area is likely consumed by the short range U-fiber system which is difficult to assess with dMRI.

The volume of hemispheric white matter (WM) occupied by axons between cortical parcels is equal to the sum of all axons' lengths multiplied by their cross-sectional areas. The mean fiber tract lengths of connections were taken from our prior dMRI analysis (3). For the effective cross-sectional area of axons we again used the inverse of the callosal fiber density (5). So calculated, the volume occupied by cortico-cortical and hippocampo-cortical fibers is $4.3x10^5$ mm^3, or about 96% of the total MRI-assessed WM volume. This implies that the number of long-range fibers cannot be larger than our estimate unless the callosal fiber density measurement is mistakenly low. The remaining WM volume may seem insufficient for connections with subcortical structures. However, the major subcortical structures known to communicate with the cortex (thalamus, amygdala, striatum, nucleus basalis, locus coeruleus, etc.) contain, in sum, less than 1% of the number of cortical neurons (8, 9). Even under the unlikely assumption that all excitatory thalamic neurons project to all cortical parcels proportionally to their area, their axons would only comprise ~4% of the total WM volume (see *Extended Methods* for calculations).

Our method has limited opportunities for error. EM determinations of human callosal fiber density are rare but consistent across studies and with light-microscopy; mis-estimated tissue shrinkage is possible but likely to be <10%. Callosal areas were measured with a well-validated widely-used method (4). Application of the callosal scaling factor to intra-hemispheric connections assumes that dMRI is equally effective at measuring intra- and inter-hemispheric connections, a reasonable assumption as the dMRI procedures were identical for intra- and interhemispheric connections, and we found only modest differences in the distance-matched dMRI connectivity for callosal versus ipsilateral connections (Fig. 1*C*).

The simple scaling factor we derive here permits some interesting quantitative estimates which may inform models of cortical neurophysiology. For example, the connections between Wernicke's and Broca's areas are thought to integrate receptive and expressive aspects of language, but there are only ~25,000 axons between the core cortical parcels in these regions (parcels 44 and PSL), fewer than the number of words in a college student's vocabulary (10). Areas distant from the hippocampus, notably the dorsolateral prefrontal cortex, may be connected to it by <10 axons/mm^2 (fig. 1*F*). On a global scale, we estimate the total number of inter-areal axons as

1.05×10^9, implying that <5% of the ~11.5×10^9 cortical pyramidal cells (11) project outside their area (because only half of the axons are efferent). Furthermore, since 51% of those are to adjacent areas, <2.5% of pyramidal cells project beyond the adjacent parcel. This sparse long-range connectivity is consistent with the exponential fall-off measured with dMRI in humans and histologically in other mammals (3, 12).

These constraints encourage consideration of models of cortical function where connections are dense but mainly local. Neural models with multiple paths between cortical neurons due to numerous short connections can show long-range covariance and even synchrony (13, 14), and these have been observed experimentally in humans (15). In such models, cortical locations interact through activation of multi-synaptic pathways rather than direct connections, and the key to connectivity is physiological selection under multiple constraints rather than anatomical projections. Lastly, it is useful to note that these quantitative considerations are radically different in other species, where the smaller number of cortical neurons and shorter inter-areal distances allow greater connectivity between cortical areas, as well as a larger proportion of subcortical connectivity.

Extended Methods

Detailed methods are provided in *SI Extended Methods*.

Acknowledgements

This work was supported by National Institutes of Health grants RF1MH117155 and R01NS109553. Data were provided, in part, by the Human Connectome Project, WU-Minn Consortium (Principal Investigators: David Van Essen and Kamil Ugurbil; 1U54MH091657) funded by the 16 National Institutes of Health (NIH) Institutes and Centers that support the NIH Blueprint for Neuroscience Research; and by the McDonnell Center for Systems Neuroscience at Washington University.

Data availability

The processed data used in this study are available at https://doi.org/10.5281/zenodo.4910310. Datafiles are in Matlab v7.3 format. The Human Connectome Project's raw imaging data and FreeSurfer outputs may be downloaded from https://db.humanconnectome.org.

Code availability

The main standalone analysis Matlab code used in this study is available at https://doi.org/10.5281/zenodo.4910310. Additional non-standalone supporting code will be made available upon request.

References

1. N. Geschwind, Disconnexion syndromes in animals and man. *Brain* **88**, 237–294 (1965).
2. Y. Assaf, H. Johansen-Berg, M. Thiebaut de Schotten, The role of diffusion MRI in neuroscience. *NMR Biomed.* **32**, e3762 (2019).
3. B. Q. Rosen, E. Halgren, A Whole-Cortex Probabilistic Diffusion Tractography Connectome. *eNeuro* **8**, ENEURO.0416-20.2020 (2021).
4. B. Fischl, FreeSurfer. *Neuroimage* **62**, 774–781 (2012).
5. F. Aboitiz, A. B. Scheibel, R. S. Fisher, E. Zaidel, Fiber composition of the human corpus callosum. *Brain Res.* **598**, 143–153 (1992).
6. M. F. Glasser, *et al.*, A multi-modal parcellation of human cerebral cortex. *Nature* **536**, 171–8 (2016).
7. A. Schüz, V. Braitenberg, The human cortical white matter: quantitative aspects of cortico-cortical long-range connectivity. *Cortical areas Unity Divers.*, 377–385 (2002).
8. P. Arcelli, C. Frassoni, M. C. Regondi, S. De Biasi, R. Spreafico, GABAergic neurons in mammalian thalamus: a marker of thalamic complexity? *Brain Res. Bull.* **42**, 27–37 (1997).
9. T. A. Avino, *et al.*, Neuron numbers increase

in the human amygdala from birth to adulthood, but not in autism. *Proc. Natl. Acad. Sci.* **115**, 3710–3715 (2018).
10. M. Brysbaert, M. Stevens, P. Mandera, E. Keuleers, How Many Words Do We Know? Practical Estimates of Vocabulary Size Dependent on Word Definition, the Degree of Language Input and the Participant's Age . *Front. Psychol.* **7**, 1116 (2016).
11. F. A. C. Azevedo, *et al.*, Equal numbers of neuronal and nonneuronal cells make the human brain an isometrically scaled-up primate brain. *J. Comp. Neurol.* **513**, 532–541 (2009).
12. X.-J. Wang, Neurophysiological and computational principles of cortical rhythms in cognition. *Physiol. Rev.* **90**, 1195–268 (2010).
13. M. Bazhenov, N. F. Rulkov, I. Timofeev, Effect of synaptic connectivity on long-range synchronization of fast cortical oscillations. *J. Neurophysiol.* **100**, 1562–1575 (2008).
14. R. Vicente, L. L. Gollo, C. R. Mirasso, I. Fischer, G. Pipa, Dynamical relaying can yield zero time lag neuronal synchrony despite long conduction delays. *Proc. Natl. Acad. Sci.* **105**, 17157 LP – 17162 (2008).
15. C. W. Dickey, *et al.*, Widespread ripples synchronize human cortical activity during sleep, waking, and memory recall. *bioRxiv*, 2021.02.23.432582 (2021).

Supporting Information: Extended Methods

Diffusion MRI

The dMRI connectivity data used to estimate inter-parcel axon totals was described in our prior report (3) whose data are available in full at https://doi.org/10.5281/zenodo.4060485. Preprocessed imaging data for 1,065 healthy young adults were retrieved from the Human Connectome Project WU-Minn consortium 1200 release (16) (https://db.humanconnectome.org). We segmented the cortex into 180 parcels per hemisphere following the HCP-MMP1.0 atlas(6) and performed probabilistic tractography using the probtrackX tool (17) from FSL (18) using tractography parameters detailed in our prior report (3). This analysis yielded a 360 x 360 dMRI connectivity matrix for each subject which provided the example data for applying the method presented here. For probtrackX-derived connectivity, the raw unit of dMRI connectivity strength is the number of streamlines connecting seed and target regions. The absolute magnitude of this metric is arbitrary as it scales with the number of samples drawn from the probability distribution of diffusion parameters in each voxel, in our analysis 5,000. Note that the method described here is largely agnostic to the dMRI methodology, provided it returns a continuous connectivity metric and has relatively equal sensitivity to callosal and ipsilateral connections.

Cross-sectional area of the corpus collosum, white matter volume, and parcel areas

The HCP WU-Minn consortium 1200 release (16) includes the standard outputs from the FreeSurfer `recon-all` pipline (4). With default parameters, this pipeline labels the 1 mm^3 voxels of the `aseg.mgz` volume which contain the corpus callosum with a fixed 5mm lateral extent. Dividing the number of callosum-label voxels by 5 yields an estimate of its cross-sectional area, in mm^2. The total white matter volume is reported in the `aseg.stats` output of `mri_segstats`. Parcel areas and adjacency were determined (19) on triangular mesh of each subject's reconstruct white matter surface, or white matter – gray matter interface (`?h.white`).

Estimate of callosal fiber density

Our estimate of callosal fiber density was based on the electron microscopy (EM) study of Aboitiz and colleagues (5) who reported a fiber density of 38 per 100 μm^2 or 1.6×10^5 axons/mm^2 after

accounting for 65% linear tissue shrinkage after fixation. This is concordant with their finding of 1.57×10^5 axons/mm^2 as measured with light-microscopy in twenty brains as well as the 1.23×10^5 non-exhaustively counted axons per mm^2 reported in a more recent EM study (20) of callosal axon diameter in two brains (20), assuming the same degree of tissue shrinkage.

Distance matched Intra- vs. Interhemispheric dMRI connectivity

One assumption of the method described in this report is that the dMRI tractography methodology has approximately similar sensitivity to callosal and ipsilateral connections. This is difficult to determine without ground truth connectivity, as intra- and interhemispheric connections may have true anatomical differences. Nevertheless, we examined distance-matched intra- vs interhemispheric connection and found them qualitatively similar, see Fig. 1*C*.

Estimating axon counts and axon volume from dMRI

From the histological estimate of callosal fiber density, MRI-derived measures of callosal cross-sectional area and white matter connectivity, the conversion factor between dMRI connectivity and physical axons can be estimated as follows:

Eq. 1.1 $N_{callosum} = A_{callosum} * D_{callosum}$

Eq. 1.2 $C_{axon} = \frac{Ncallosum}{M_{dMRI}}$

Where $A_{callosum}$ is the cross-sectional area (mm^2), $D_{callosum}$ is the assumed fiber density (1.6×10^5 axons/mm^2) of the corpus callosum, $N_{callosum}$ is the estimated total number of callosal fibers, M_{dMRI} is the magnitude of dMRI callosal connectivity, in our case, the number of tractography streamlines, and C_{axon} is the conversion factor from dMRI to physical fibers (axons/streamline).

In addition to connectivity strength, or number of streamlines, the dMRI tractography analysis also yields a mean streamline length for every parcel-pair connection. After converting dMRI connectivity strength to physical axon count as described above, the total volume of the estimated axons can be calculated as follows:

Eq. 2.1 $WM_{volume} = \sum_{i=1}^{N_{pair}} l_i * n_i * C_{axon} * \frac{1}{D_{callosum}}$

Eq. 2.2 $WM_{volume} = \sum_{i=1}^{N_{pair}} l_i * n_i * \frac{A_{callosum}}{M_{dMRI}}$

Where WM_{volume} is the estimated axonal white matter volume (mm^3) and N_{pair} is the total number of parcel pairs. l_i and n_i are the length (mm) and number of dMRI streamlines in the ith parcel pair. Eq. 2.1 can be simplified into Eq. 2.2 by substituting Eqs. 1.1 and 1.2 into 2.1.

Parcel ordering

The parcel ordering and the ten functional networks shown in Fig 1*A* were defined in our previous report (3) and were modified from twelve networks identified by Ji and colleagues in a resting-state fMRI study on the HCP cohort (21).

Thalamocortical fiber volume estimation

The scope of our previous dMRI tractography study (3) was confined to corticocortical (including cortico-hippocampal) connectivity. In order to estimate the total volume of thalamocortical axons, we assumed a total axon count of 22.6×10^6 as reported by histological count (8) and allocated these axons to cortical parcels in proportion to their area. The inverse callosal packing density was used for effective cross-sectional area, as with corticocortical connections. To estimate the length of

thalamocortical fiber tracts, for each parcel i, we first identified the thalamic voxel nearest to parcel's centroid. We then used the interparcel fiber tract length (3) from the centroid of parcel i to the identified parathalamic parcel centroid. To this figure we added the Euclidean distance from the parathalamic centroid to the nearest voxel of the thalamus, ensuring that estimated thalamocortical fiber tract length is always non-zero. As with corticocortical connections, the total white matter volume of each connection was estimated by taking the product of the number of axons, the effective cross-sectional area, and the estimated fiber tract length (Eq. 2).

References

1. B. Q. Rosen, E. Halgren, A Whole-Cortex Probabilistic Diffusion Tractography Connectome. *eNeuro* 8, ENEURO.0416-20.2020 (2021).
2. D. C. Van Essen, *et al.*, The WU-Minn Human Connectome Project: An overview. *Neuroimage* 80, 62–79 (2013).
3. M. F. Glasser, *et al.*, A multi-modal parcellation of human cerebral cortex. *Nature* 536, 171–8 (2016).
4. T. E. J. Behrens, H. J. Berg, S. Jbabdi, M. F. S. Rushworth, M. W. Woolrich, Probabilistic diffusion tractography with multiple fibre orientations: What can we gain? *Neuroimage* 34, 144–155 (2007).
5. M. Jenkinson, C. F. Beckmann, T. E. J. Behrens, M. W. Woolrich, S. M. Smith, FSL. *Neuroimage* 62, 782–790 (2012).
6. B. Fischl, FreeSurfer. *Neuroimage* 62, 774–781 (2012).
7. M. Meyer, M. Desbrun, P. Schröder, A. H. Barr, "Discrete Differential-Geometry Operators for Triangulated 2-Manifolds" in (2003), pp. 35–57.
8. F. Aboitiz, A. B. Scheibel, R. S. Fisher, E. Zaidel, Fiber composition of the human corpus callosum. *Brain Res.* 598, 143–153 (1992).
9. D. Liewald, R. Miller, N. Logothetis, H. J. Wagner, A. Schüz, Distribution of axon diameters in cortical white matter: an electron-microscopic study on three human brains and a macaque. *Biol. Cybern.* 108, 541–557 (2014).
10. J. L. Ji, *et al.*, Mapping the human brain's cortical-subcortical functional network organization. *Neuroimage* 185, 35–57 (2019).
11. P. Arcelli, C. Frassoni, M. C. Regondi, S. De Biasi, R. Spreafico, GABAergic neurons in mammalian thalamus: a marker of thalamic complexity? *Brain Res. Bull.* 42, 27–37 (1997).